Proceedings of the 17th World Congress
The International Federation of Automatic Control
Seoul, Korea, July 6-11, 2008

Fully automatic taxiing, takeoff and landing of a UAV based on a single-antenna GNSS receiver

Am Cho, Jihoon Kim, Sanghyo Lee, Bosung Kim, Noha Park, Dongkeon Kim, Changdon Kee

School of Mechanical and Aerospace Engineering, Seoul National University,
Seoul, Korea, (e-mail: cho1838, tbaseotw, ryanlee, kbs446, noha8117, kdk3971, kee @snu.ac.kr)}

Abstract: This paper presents fully automatic control of an unmanned aerial vehicle (UAV) from taxiing and takeoff to landing based on a single-antenna GPS receiver. In this paper, inertial sensors such as gyros and accelerometers are not used at all to show the full potential of a single-antenna GPS receiver based attitude determination system. DGPS is implemented to give high accuracy position information for automatic taxiing, landing and takeoff on the runway. For a fixed wing aircraft, under the assumption of coordinated flight, the attitude information called as pseudo-attitudes can be estimated from the measurements of a single-antenna GPS receiver. Therefore full state variables for the automatic control can be obtained from single-antenna GPS receiver. In addition to GPS receiver, only an airspeed sensor is added because the velocity relative to the air is very important during landing and takeoff. The forward velocity is replaced with the airspeed obtained from Pitot tube. From linearized equations of motions around the steady state, LQR controllers for takeoff and landing are built. In particular, the flare controller that controls the pitch, altitude and airspeed of a UAV is designed. During flight tests, the aircraft taxies and takes off the runway, follows the predefined waypoint path, and then lands on the runway along the curved approach path, all fully automatically. Based on flight test results, a single-antenna GPS receiver can be used as a main sensor for a backup or a low-cost control system of UAVs

1. INTRODUCTION

GPS (Global Positioning System) receivers and IMU (Inertial Measurement Unit) are widely used as the sensors for navigation and control of unmanned aerial vehicles (UAVs). Inertial sensors have good dynamic characteristics and short-term stability, but its solutions degrade without bound over time. An INS (Inertial Navigation System) might be very expensive in order to obtain accurate position information. In addition, initialization and alignment problems must be solved. Therefore inertial sensors usually used with other external sensors. On the other hand, a GPS receiver can usually give position, velocity, and time information and its solutions are highly accurate with bounded errors, independent of time. Although GPS receivers could be vulnerable to external environments, they are widely used due to their simple and convenient usage and low cost with high accuracy. Also GPS keeps being modernized and other satellite navigations such as GALILEO and GLONASS are under development. Thus accuracy, integrity, availability and continuity of satellite navigations systems will be more improved.

A single-antenna GPS receiver usually gives time, position, and velocity information. However, for a fixed wing aircraft, the attitude information can be estimated from the measurements of a single-antenna GPS receiver [1]-[2]. This attitudes information makes it possible to use a GPS receiver as a main sensor for navigation and control of a UAV. This paper addresses automatic takeoff and landing and taxiing of a UAV based on a single-antenna GPS receiver only. In this paper, no inertial sensors such as gyros and accelerometers are used to show the full potential of a single-antenna GPS receiver based attitude system. In addition to GPS receiver, only an airspeed sensor is added because the velocity relative to the air is very important during landing and takeoff. And DGPS is implemented to give high accuracy position information for automatic landing on the runway. During flight tests, the aircraft taxies and takes off the runway, follows the predefined and/or real-time commanded waypoint path, and then lands on the runway along the curved approach path, all fully automatically.

2. SINGLE-ANTENNA GPS ESTIMATOR

A single-antenna GPS receiver usually gives position and velocity measurements, but it was shown by Kornfeld et al. that the aircraft attitude can be estimated from the velocity measurements of a single-antenna GPS receiver [1]. Their key contribution is to estimate the “pseudo-roll” angle. The aircraft acceleration vector is estimated from GPS velocity measurements using Kalman filter. It is assumed that the lift acceleration vector l is equal to the vector difference of normal components of the aircraft acceleration vector and the gravitational acceleration vector perpendicular to the velocity vector. Then the roll angle is determined by complementary angle between pseudo-lift angle acceleration vector l and the horizontal reference vector the vector $\mathbf{p}$ as shown in Figure 1.

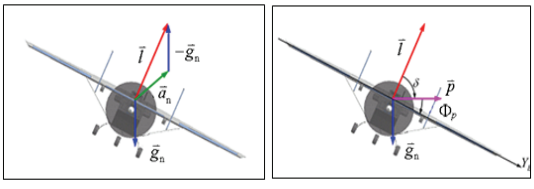

Fig. 1. Roll angle determination

Single-antenna based attitudes also can be obtained using the direction cosine matrix by introducing a new body frame [2]. From the measurements of a single-antenna GPS receiver, the NED-axis components of the specific force vector can be determined by

$$f^n = a^n - g^n \tag{1}$$

Then, by defining the single-antenna frame such that the velocity vector coincides with its x-axis and the specific force vector lies in its x − z plane, we have the coordinate transformation C_n^b from the NED frame to the single-antenna frame, given by

$$C_n^b = \begin{bmatrix} \hat{v}^n & \hat{v}^n \times \hat{f}_\perp^n & -\hat{f}_\perp^n \end{bmatrix}^T \tag{2}$$

Where $\hat{v}^n = \dfrac{v^n}{|v^n|}$, $\hat{f}_\perp^n = \dfrac{f_\perp^n}{|f_\perp^n|}$ and $f_\perp^n = f^n - (f^n \bullet \hat{v}^n)\hat{v}^n$

Then from the relation between the direction cosine matrix and Euler angles, the attitude of the single-antenna frame with respect to the NED frame can be represented by the Euler angles, which are given by

$$\Phi = \tan^{-1}\left(\frac{\hat{v}_N(\hat{f}_\perp)_E - \hat{v}_E(\hat{f}_\perp)_N}{-(\hat{f}_\perp)_D}\right)$$

$$\Theta = \sin^{-1}(-\hat{v}_D) \tag{3}$$

$$\Psi = a\tan 2(\hat{v}_E, \hat{v}_N)$$

where

$$\hat{v}^n = \begin{bmatrix} \hat{v}_N & \hat{v}_E & \hat{v}_D \end{bmatrix}^T \text{ and } \hat{f}_\perp^n = \begin{bmatrix} (\hat{f}_\perp)_N & (\hat{f}_\perp)_E & (\hat{f}_\perp)_D \end{bmatrix}^T$$

The Euler angle rates $(\dot{\Phi}, \dot{\Theta}, \dot{\Psi})$ can be obtained by time differencing of filtering the Euler angles. Then the angular velocities (P,Q,R) are determined from the coordinate transformation. Since the x axis of the single-antenna frame is defined to coincide with the aircraft velocity vector, the body-axis component of the velocity vector can be determined by

$$U = \sqrt{v_N^2 + v_E^2 + v_D^2}$$

$$V = W = 0 \tag{4}$$

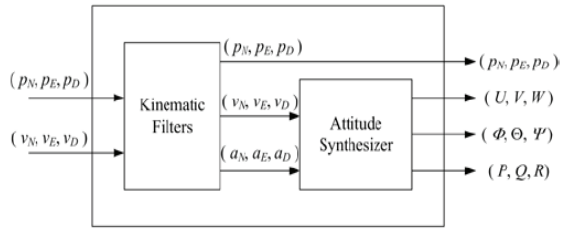

Fig 2. Single-Antenna GPS Estimator

If an airspeed sensor is available, forward velocity U can be replaced with the airspeed obtained from Pitot tube. In this paper, the airspeed from Pitot tube was used for the automatic control of UAV during flight tests.

3. CONTROLLER DESIGN

For designing linear controllers, the nonlinear equations of motion should be linearized around the steady-state trajectories. When the total velocity V_T, vertical flight path angle γ, and yaw rate $\dot{\Psi}$ are given under the assumption of steady coordinated flight, the trim values of the state and input variables can be computed.

A linear system, given by the linearized equations of motion, is represented by

$$\dot{x} = Fx + Gu \tag{5}$$

where the input vector u is given by

$$u = [\delta_e \quad \delta_t \quad \delta_a \quad \delta_r]^T \tag{6}$$

For path control, the state vector is given by

$$x = [u \quad w \quad q \quad \theta \quad d \quad v \quad r \quad p \quad \phi \quad \psi \quad y]^T \tag{7}$$

The error states, which are heading error ψ, cross track error y, and altitude error h are not related to the trim conditions and thus they do not affect the trim inputs. The error states can be defined as the deviations from the commanded values, and how to compute them depends on the output commands such as altitude, heading, and path control commands.

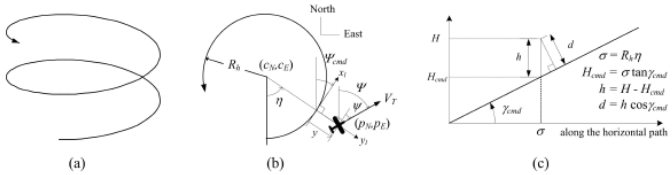

Fig. 3. Computation of tracking errors (ψ, y, h, d) : (a) A 3-dimensional helical path, (b) Horizontal projection, (c) Vertical projection along the horizontal path

For helical path control, as shown in Fig. 3, the error states can be defined as the deviations from the commanded values of the intersection point between the path and the radial vertical plane passing through the current aircraft position:

$$\psi = \Psi - \Psi_{cmd}$$

$$y = \sqrt{(p_N - c_N)^2 + (p_E - c_E)^2} - R_h \tag{8}$$

$$h = H - H_{cmd}$$

where

$$\Psi_{cmd} = a\tan 2(p_E - c_E, p_N - c_N) - \pi/2$$

$$H_{cmd} = \sigma \tan \gamma_{cmd} \quad (9)$$

and (c_N, c_E) and R_h are the horizontal center and radius of the helical path. σ is the horizontal arc length along the horizontal path and γ_{cmd} is the vertical flight path angle along the helical path. For path control, the vertical slope track d is used instead of the altitude error h :

$$d = h \cos \gamma_{cmd}$$

We use Linear Quadratic Regulator (LQR) control laws in designing linear controllers. An LQR control problem is to find an optimal gain matrix C such that the state-feedback law

$$u(t) = -Cx(t) \quad (10)$$

minimizes the performance index given by

$$J = \int_0^\infty (x^T Ax + u^T Bu)dt \quad \text{subject to Eq. (10).}$$

Here, design parameters are weighting matrices A and B, which affect the performance of the controller. Note that for given F, G, A and B, it is easy to compute the optimal gain matrix C by using modern software such as MATLAB. The weighting matrices A and B are usually obtained through many simulations [6], [11].

In summary, the control input vector U could be considered as the sum of the trim input vector U_1 and the perturbed input vector u , given by $U = U_1 + u$. U_1 can be obtained from the trim conditions and u can be obtained by the LQR controller. The longitudinal controllers include climb-rate, altitude, glide slope controllers, whereas the lateral controllers include bank, heading, line track, and circle track controllers. Figure 4 shows the block diagram of an overall control logic where trim processes are introduced before and after applying the linear control law. By switching gain matrices corresponding to the state, input and output vectors, various controllers can be executed.

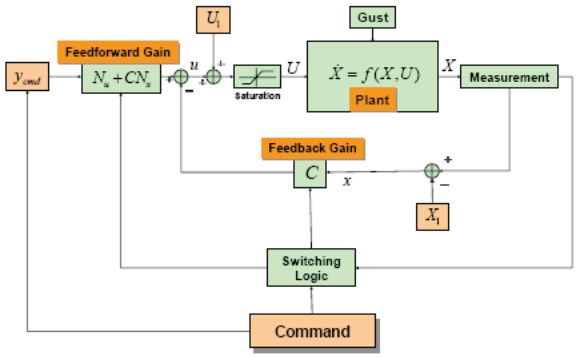

Fig. 4. Block diagram of overall control logic

3.1 Automatic Taxiing

For the taxiing on the runway, a path tracking controller was designed. This controller can be used before takeoff or after landing. The dynamics during taxiing is modeled as a common car-like vehicle with a single steering under the assumption of point-mass and slippage-free motion [13]. The Path-tracking controller is made up of a steering controller and a speed controller. If the desired tracking velocity is constant, the steering controller can be designed by linear quadratic regulator control laws using a dynamic model [13]. The steering controller receives as input the heading, lateral and steering offsets and gives as output the steering rate. The taxiing path is generated from commanded or pre-defined waypoints using Dubin's set. Because the heading information is obtained only by GPS receiver, the steering control is possible above a ground speed threshold. The maximum steering angle is limited based on the taxiing speed to avoid a rollover. The speed controller has the structure of a PI controller.

3.2 Automatic Takeoff

Automatic takeoff controller is made up of the runway track and climbout controller. Runway track controller maintains the UAV alignment with the runway centerline. During rolling, the process to keep from the rollover of UAV is added. Climbout controller controls climb rate of the UAV using elevator with full throttle. The lift off is decided from airspeed and climb rate. Climbout is completed when the UAV achieves a pre-specified altitude and longitudinal controller is switched to an altitude controller.

3.3 Automatic Landing

In the flare mode, airspeed, pitch, and altitude are controlled. The output vector of a flare controller is as follows:

$$y_c = [u \quad \theta \quad h]^T$$

Because the number of outputs exceeds the number of controls, this controller determines the input variables that produce the smallest output error. So appropriate output commands need to be activated for the moderate touchdown. These commands are decided through simulation and flight tests. In simulation and flight test, during flare, it was observed that elevator input oscillates with the period of short-period mode. Note that single-antenna GPS based estimator doesn't provide true pitch. The pseudo-pitch is a vertical fight-path angle in fact. This oscillation was solved by applying a low-pass filter to an elevator input. The time constant of a filter was set to the period of short-period mode.

4. SYSTEM CONFIGURATION

Commercial off-the-shelf (COTS) PC/104 modules are used as a flight control computer. To measure airspeed, pressure sensor is connected to PC104 A/D module. The dynamic pressure is sampled at 100 kHz. A wireless modem and GPS receiver are connected to PC104 serial communication expansion stack. Novatel 3151R GPS receivers are used for

both reference and user GPS receivers. The maximum output rate of the used GPS receiver is 10 Hz.

Fig. 5. UAV used in the flight test

The programming environment for both onboard and ground computers is Microsoft Windows XP professional and Visual C++ with MFC. Windows OS is not a real-time OS, but is good enough for the purpose of verifying our automatic flight control system. Data communications between programs in onboard or ground computers are achieved through Ethernet network by using UDP (User Datagram Protocol), whereas onboard and ground computers communicate through wireless modems by using RS232 serial communications.

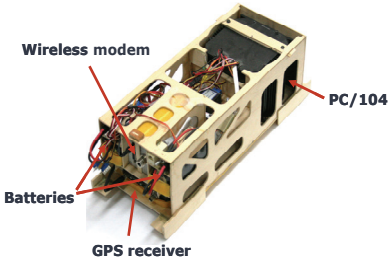

Fig. 6. The payload box

An overview of flight control system of UAV is shown in the following figure 7.

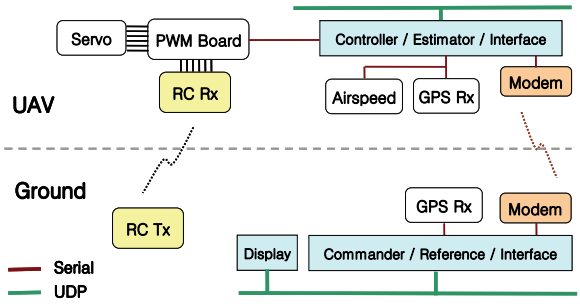

Fig. 7. Schematic of automatic flight control system

5. FLIGHT TEST RESULTS

In this paper, the main sensor of the UAV is a single-antenna GPS receiver and full states of UAV are obtained from single-antenna GPS based estimator. Inertial sensors such as gyros and accelerometers are not used at all except for single-antenna GPS receiver and airspeed sensor. To improve the robustness to wind effects, the forward velocity of the UAV is replaced with the airspeed measured from the Pitot tube. DGPS reference station was implemented at the ground station to improve the position accuracy.

The single-antenna GPS estimator starts to estimate attitude information when the UAV velocity becomes more than the pre-specified value, say, 3 m/s. This velocity value is reached shortly after the UAV starts to move. During this period, attitude is not fed back. When the UAV rolls on the runway, steering control is added. In fact, takeoff rolling is done in a very short time period. During takeoff, climb-rate control is used for the longitudinal control with full throttle power and heading control is used for the lateral control.

After the UAV reaches the design altitude, waypoint path control is used. For horizontal path control, line and circle track controllers are used for linear and circular paths, respectively. For vertical path control, there are two modes: altitude control and vertical slope track control. Most of time, altitude control mode is used. Vertical slope track control is used for glide slope control. Flare control uses forward speed/pitch/altitude. To improve the steady-state errors, integrators are used on the velocity and position tracking errors. The aircraft velocity is regulated around 26 m/s except for takeoff and landing.

Fig. 8-10 show 3-dimensional, horizontal, and vertical trajectories of fully automatic control of the UAV from takeoff to landing. The UAV starts to roll along the runway at A and takes off shortly after. When the UAV reaches the altitude 70 m, it has a smooth transition interval of 3 sec. Then, waypoint path control is activated at B. After that, at C, it starts to descend, following a curved glide slope approach path with the glide slope angle of 3 deg. Finally, the UAV performs flare control at D and then touches down on the runway. Only one command is uplinked to the UAV by clicking buttons at A. Commanded paths are dotted lines. There was a wind of 2–3 m/s at the ground level. As shown in Fig. 10, it is seen that altitude control yields altitude error of about 3 m due to wind effects, which can be eliminated if wind information is known. Actual trajectories in the linear glide slope path converge to the command path due to the effects of integrators. This is clearly shown in Fig. 12. Horizontal cross track errors converge to within 3-4 m and vertical slope track errors converge to within 0.5 m. Due to the limit of DGPS vertical positioning accuracy, ground levels of touch down points were not consistent during several experiments in Fig. 11. However, it can be overcome by careful design of the flare control system.

Fig. 13-14 shows taxiing experiment results on the ground. Taxiing path is generated from pre-defined waypoints using Dubin's set. In Fig. 13, UAV follows the initial path generated in real time to reach commanded path due to large initial heading error. Taxiing speed was set to 1.5m/s. Because the single-antenna GPS receiver is the only sensor during taxiing, steering control is started when the ground speed of the UAV goes above threshold 0.5m/s. There was a wind of 4-5 m/s at the ground level during taxiing. Due to the wind, the maximum ground speed was about 1.6m/s in downwind and minimum ground speed was about 0.5m/s in upwind. Maximum lateral offset was within 2m in the rear wind. The performance of ground speed control of the UAV

was not marginally satisfied, which will be improved by throttle gain tuning in the future.

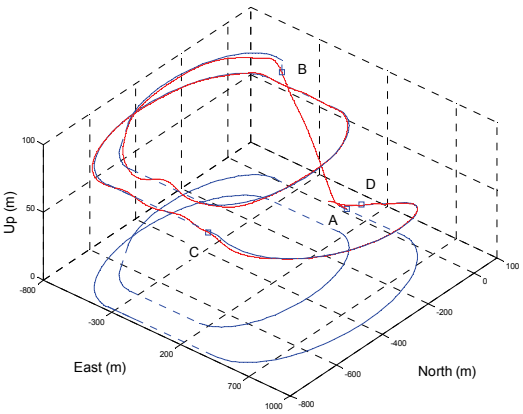

Fig. 8. 3D trajectory of flight test

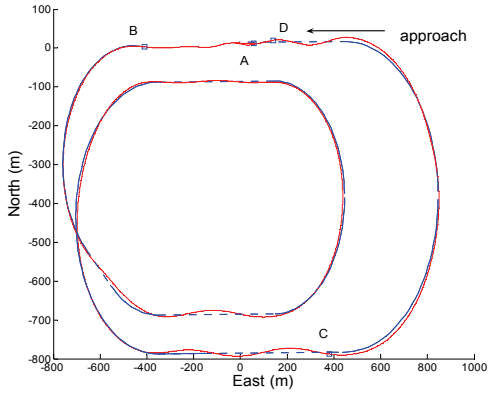

Fig. 9. 2D horizontal trajectory of flight test

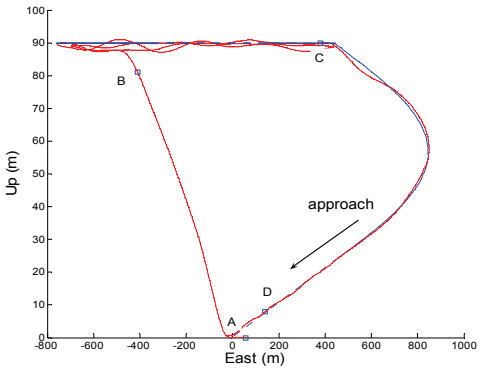

Fig. 10. Vertical trajectory

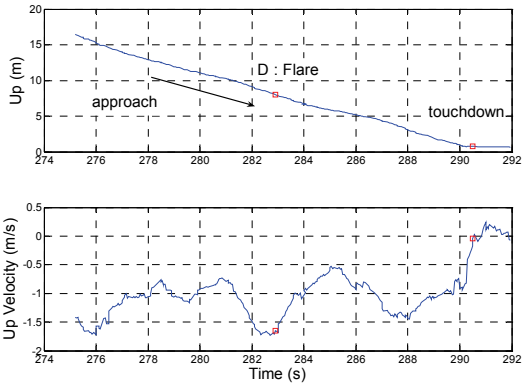

Fig. 11. Vertical time history and Up velocity

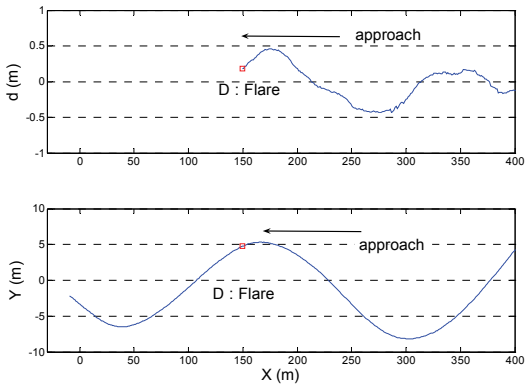

Fig. 12. Position tracking errors during automatic landing

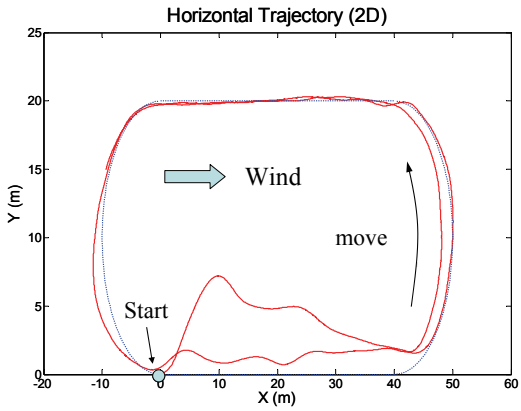

Fig. 13 Horizontal trajectory during taxiing

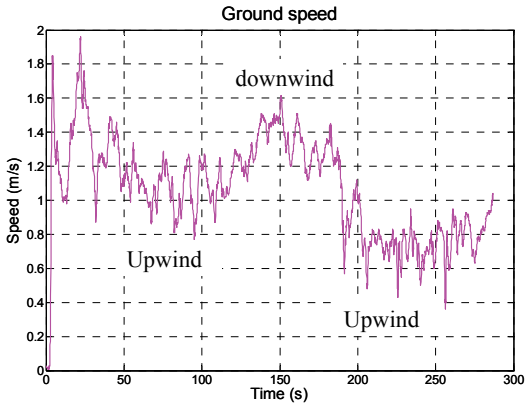

Fig. 14 Ground velocity during taxiing

6. CONCLUSIONS

We presented the methods of designing an estimator and controllers to use a single-antenna GPS receiver as a primary sensor for a UAV. Differential GPS (DGPS) is used to obtain high accuracy position information. To improve the robustness to wind effects, the forward velocity of the UAV is replaced with the airspeed measured from the Pitot tube. No inertial sensors such as gyros and accelerometers are used. Flight test results showed that the automatic control a UAV from taxiing and takeoff to landing by using a single-antenna GPS receiver and airspeed sensor only was sufficient. Based on the results, a single-antenna GPS receiver can be sufficiently used as a main sensor for a backup or a low-cost control system of UAVs. In the future work, wind estimation algorithm will be used to improve the robustness to wind effects [10]. To decide flare altitude and touchdown, a low-cost ultrasonic altimeter or carrier-phase DGPS can be used.

REFERENCES

[1] Kornfeld, R.P., Hansman, R.J., and Deyst, J.J., "Single-Antenna GPS-Based Aircraft Attitude Determination", *Journal of the Institute of Navigation*, vol.45, pp.51-60, Spring 1998.

[2] S. Lee, A. Cho, J. Kim, and C. Kee, "Fully Automatic Control from Takeoff to Landing of a UAV Based on a Single-Antenna GPS Receiver", *AUVSI's Unmanned Systems North America 2006*, Sep. 2006

[3] Lee, S., Kim J., Cho A., Cheong H., Kee, C., "Developing an Automatic Control System of Unmanned Aircrafts with a Single-Antenna GPS Receiver" *Proceeding of the ION GNSS-2004*, 2004.

[4] Lee, S., Lee, T., Park, S., Kee, C., "Flight Test Results of UAV Automatic Control Using a Single-antenna GPS receiver", AIAA GN&C Conference and Exhibit, 2003.

[5] Brown and Hwang, *Introduction to Random Signals and Applied Kalman Filtering*, John Wiley & Sons, Inc., 1997.

[6] Bryson Jr., A.E., *Control of Spacecraft and Aircraft*, Hemisphere, New York, 1995.

[7] Jaegyu Jang, and Changdon Kee, "Flight Test of Attitude Determination System using Multiple GPS Antennae," *Journal of Navigation*, vol. 59, No. 1, Jan, 2006, pp. 119-133.

[8] Kee, C., Park, S., et al., "Flight Test of Helicopter Landing System using Real-time DGPS," *Proceedings of the ION GPS-99*, 1999.

[9] P.Y. Montgomery, "Carrier Differential GPS as a Sensor for Automatic Control" Ph.D. Thesis, Stanford University, 1996.

[10] Am Cho, Jihoon Kim, Sanghyo Lee and Changdon Kee, "Wind Estimation and Airspeed Calibration Using the UAV with a Single-Antenna GNSS Receiver and Airspeed Sensor", *IEEE Transactions on Robotics*, submitted for publication.

[11] F. L. Lewis, *Applied Optimal Control & Estimation*, Englewood Cliffs, NJ: Prentice Hall, 1992.

[12] B. L. Stevens and F. L. Lewis, *Aircraft Control and Simulation*, New York: Wiley-Interscience, 1992.

[13] R. M. DeSantis, "Path-Tracking for Car-Like Robots with Single and Double Steering", *IEEE Transactions on vehicular technology*, vol. 44, May 1995

[14] Robert C. Nelson, *Flight Stability and Automatic Control*, WCB/McGraw-Hill, 1998.